



Published in final edited form as:

ACS Chem Neurosci. 2023 July 19; 14(14): 2569–2581. doi:10.1021/acchemneuro.3c00268.

## Peptidomic analysis reveals seasonal neuropeptide and peptide hormone changes in the hypothalamus and pituitary of a hibernating mammal

Somayeh Mousavi<sup>1</sup>, Haowen Qiu<sup>2,3</sup>, Matthew T. Andrews<sup>4,\*</sup>, James W. Checco<sup>1,3,\*</sup>

<sup>1</sup>Department of Chemistry, University of Nebraska-Lincoln, Lincoln, NE 68588, United States

<sup>2</sup>Center for Biotechnology, University of Nebraska-Lincoln, Lincoln, NE 68588, United States

<sup>3</sup>The Nebraska Center for Integrated Biomolecular Communication (NCIBC), University of Nebraska-Lincoln, Lincoln, NE 68588, United States

<sup>4</sup>School of Natural Resources, University of Nebraska-Lincoln, Lincoln, NE 68583, United States

### Abstract

During the winter, hibernating mammals undergo extreme changes in physiology which allow them to survive several months without access to food. These animals enter a state of torpor, which is characterized by decreased metabolism, near-freezing body temperatures, and a dramatically reduced heart rate. The neurochemical basis of this regulation is largely unknown. Based on prior evidence suggesting that the peptide-rich hypothalamus plays critical roles in hibernation, we hypothesized that changes in specific cell-cell signaling peptides (neuropeptides and peptide hormones) underlie physiological changes during torpor/arousal cycles. To test this hypothesis, we used a mass spectrometry-based peptidomics approach to examine seasonal changes of endogenous peptides that occur in the hypothalamus and pituitary of a model hibernating mammal, the thirteen-lined ground squirrel (*Ictidomys tridecemlineatus*). In the pituitary, we observed changes in several distinct peptide hormones as animals prepare for torpor in October, exit torpor in March, and progress from Spring (March) to Fall (August). In the hypothalamus, we observed an overall increase in neuropeptides in October (pre-torpor), a decrease as the animal enters torpor, and an increase in a subset of neuropeptides during normothermic interbout arousals. Notable changes were observed for feeding regulatory peptides, opioid peptides, and several peptides without well-established functions. Overall, our study provides critical insight into changes in endogenous peptides in the hypothalamus and pituitary during mammalian hibernation that were not available from transcriptomic measurements. Understanding the molecular basis of the

\*Corresponding authors: matt.andrews@nebraska.edu, checco@unl.edu.

#### Author Contributions

M.T.A. and J.W.C. conceived of the study. S.M., M.T.A., and J.W.C. performed the experiments. H.Q. performed statistical analysis. All authors analyzed the data. S.M., M.T.A., and J.W.C. wrote the initial draft of the manuscript. All authors contributed to writing the final manuscript.

#### Supporting Information

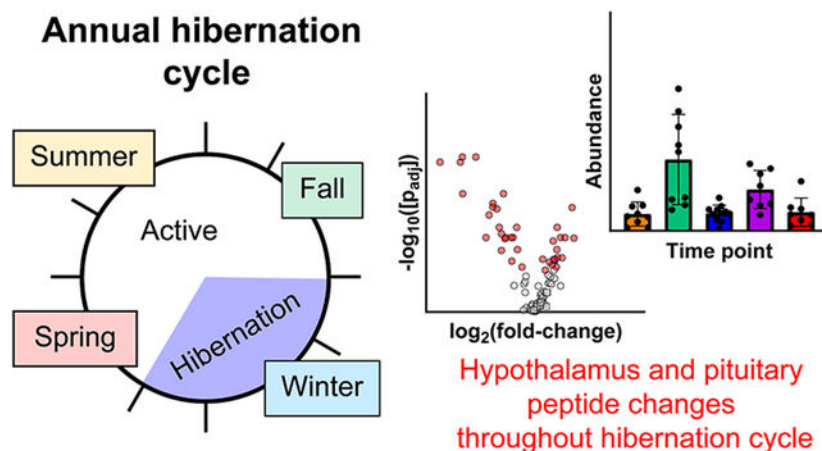
Supporting figures, including tissue freeze time, sample normalization results, heat maps, PCA with body temperatures labeled, October vs. March univariate comparison, and table of peptide functions (PDF).

Supporting tables, including peptide information, peptide peak areas, and data from univariate statistics for pairwise comparisons for each tissue (two XLSX documents).

M.T.A. is an advisor for Fauna Bio Inc. All other authors declare they have no competing interests.

hibernation phenotype may pave the way for future efforts to employ hibernation-like strategies for organ preservation, combating obesity, and treatments for stroke.

## Graphical Abstract



## Keywords

Hibernation; peptidomics; mass spectrometry; neuropeptides; peptide hormones; hypothalamus; pituitary

## Introduction

Hibernation is one of the most striking evolutionary adaptations in mammals, granting these animals the ability to cope with environmental extremes by regulating their energy consumption while their body temperature, metabolism, and heart rate are intensely depressed.<sup>1-4</sup> In small hibernating mammals such as the thirteen-lined ground squirrel (*Ictidomys tridecemlineatus*), body temperature will drop to as low as 4-5 °C, an active heart rate of 300-400 beats/minute is lowered to 5-10 beats/minute, and oxygen consumption is reduced to ~2% of the metabolically active state. This deep depression of physiological function is referred to as torpor. Throughout the hibernation season, bouts of hypothermic torpor are regularly and abruptly interrupted every 1-2 weeks by brief normothermic arousal periods lasting 12-24 hours referred to as interbout arousals (IBAs). The physiological roller coaster of long-term hypothermia and 4-6 months starvation interrupted with IBAs in the absence of feeding (Figure 1) represent a dramatic departure from normothermic homeostasis and would be lethal to most mammalian species. In particular, an IBA is initiated by a rapid explosion in heart rate and body temperature resembling reperfusion following an ischemic event. However, unlike the pathology that normally accompanies ischemia and reperfusion, hibernating mammals tolerate these extremes with no apparent injury. Many of the mechanisms underlying the preparation and maintenance of hibernation, and those that provide neuro- and cardio-protection, are largely unknown. A better understanding of the molecules and pathways that govern hibernation may lead to the utilization of hibernation strategies for treating ischemia and reperfusion injury (e.g., following stroke or myocardial infarction), organ preservation, minimizing muscle disuse

atrophy, or combating obesity.<sup>2, 4</sup> Indeed, prior studies of hibernating mammals identified melatonin and D- $\beta$ -hydroxybutyrate as playing major roles during hibernation, and follow-up studies showed that a combination of these small molecules can be used as a therapy for hemorrhagic shock.<sup>5-7</sup>

Neuropeptides and peptide hormones are endogenous cell-cell signaling molecules that regulate a variety of biological processes throughout the central nervous and endocrine systems.<sup>8-13</sup> These cell-cell signaling peptides are first synthesized by the ribosome as larger precursor proteins (prohormones) that enter the secretory pathway where they are heavily post-translationally modified to generate mature peptides for stimulation-dependent release.<sup>14-16</sup> Despite the fact that the peptide-rich hypothalamus-pituitary-adrenal and hypothalamus-pituitary-thyroid axes are known to play key roles in torpor and hibernation,<sup>2-4, 17-23</sup> relatively little is known about the roles of specific cell-cell signaling peptides in hibernators. Prior studies in this area have relied on transcript analysis,<sup>24-26</sup> which cannot provide information about the final processed forms of the peptides, or antibody-based detection methods,<sup>27-30</sup> which require preselection of peptides of interest and often cannot distinguish between similar peptides with common epitopes. Furthermore, peptide abundance is affected by rates of translation, post-translational processing, and proteolytic degradation, which does not necessarily correlate to mRNA abundance.

We hypothesized that changes in cell-cell signaling peptides from the hypothalamus and pituitary may be responsible for regulating critical physiological changes during the hibernation season. To test this hypothesis, we applied a non-targeted liquid chromatography-mass spectrometry (LC-MS) and LC-tandem mass spectrometry (LC-MS/MS) “peptidomics” approach<sup>15, 31-34</sup> to identify and quantify endogenous neuropeptides and peptide hormones as a function of season and hibernation stage in the thirteen-lined ground squirrel. LC-MS and LC-MS/MS-based peptidomics allows the detection, identification, and quantification of peptides without preselection, allowing for findings not possible with targeted antibody-based methods. Our results reveal seasonal changes in specific endogenous peptides from both the pituitary and hypothalamus, providing key insights into the dynamics of cell-cell signaling molecules during the dramatic physiological changes associated with the hibernation phenotype. These peptides likely play critical roles in the induction and maintenance of hibernation, and may contribute to the neuroprotective effects during the rapid increases in heart rate and body temperature associated with IBAs.

## Results

### Study design, peptide isolation, and analysis

Thirteen-lined ground squirrels were captured near Lincoln, Nebraska during July and August and housed at ~20 °C with full access to food and water and 12:12 light:dark cycle. During summer (July-September) the animals accumulate a large amount of fat in their white adipose tissue. This period of fattening is followed by a reduction in appetite in late September and early October<sup>24</sup> along with the beginning of brief shallow bouts of torpor.<sup>35</sup> In this study we recorded October body temperatures ( $T_b$ ) of 21-35 °C at the time of sacrifice. Beginning in early November animals were moved into an environmental chamber with ambient temperature of 5 °C, 24 h dark, no food, but water was available.

Under these conditions, the animals naturally enter a state of deep torpor with  $T_b = 5-6$  °C in this study. These bouts of torpor are regularly interrupted by brief IBAs where  $T_b = 8-37$  °C in this study. To evaluate peptide dynamics in the CNS, animals were sacrificed at five different time points/activity states throughout the hibernation season (Figure 1): 1) August, when the animals are in an active state; 2) October, when the animals begin their transition into the hibernation season ( $T_b = 21-35$  °C); 3) December-January, while animals are in a deep torpid state ( $T_b = 5-6$  °C); 4) December-February, while animals are in an IBA ( $T_b = 8-37$  °C); and 5) March, when the animals are in an active post-hibernation state.

We chose to analyze the pituitary and hypothalamus because these tissues are rich in neuropeptides and peptide hormones,<sup>36-39</sup> signaling molecules that we hypothesize may be important in the induction and maintenance of the hibernation phenotype. At each of the seasonal collection points, animals were euthanized by decapitation followed by rapid removal and flash freezing of the hypothalamus and pituitary in liquid nitrogen. The average time from decapitation to freezing of the hypothalamus was  $2.6 \pm 0.4$  min for all samples, while the average time from decapitation to freezing of the pituitary was  $3.8 \pm 0.8$  min for all samples (Figure S1). Endogenous peptides were extracted from tissues using both organic and aqueous extraction steps, and enriched using molecular weight-based centrifugation filtration devices and solid-phase extraction. Extracted peptides were analyzed by a LC-MS and LC-MS/MS-based label-free peptidomics workflow,<sup>33, 34</sup> which include steps for data filtering, batch correction, imputation, and normalization (Figures S2-S5). Following data processing and normalization, relative peptide abundances were compared between groups using multivariate and univariate statistical analyses.

### Dynamics of pituitary peptides

Peptides were identified from the pituitaries of 37 animals across the five activity states (n = 5-9 per activity state). Following database identification, 342 different peptides were identified from these samples with a 1% false discovery rate (FDR). To facilitate statistical analysis, peptides with ambiguous identifications, a low number of MS/MS identifications, or a high percentage of missing values were filtered (see Methods). Following this processing, 94 pituitary peptides were deemed “present” and appropriate for statistical analysis across samples (see Supporting Document). The majority of these peptides (86/94) are from signal peptide-bearing proteins, suggesting that they arise from prohormones processed through the secretory pathway. As expected for the pituitary,<sup>36, 37, 40</sup> many of these peptides were derived from pro-opiomelanocortin (POMC), proenkephalin A (PENK), and granins.

Principle component analysis (PCA) of pituitary peptides showed clustering of each activity state, with the August active, December-January torpor, and March active group not overlapping with one another (Figure 2 and Figure S6). Interestingly, the October and December-February IBA groups showed considerable overlap with the December-January torpor and March active groups. This result is consistent with the transitional nature of these two time points in physiology as reflected in broader range of internal body temperatures. October is the period in which animals display a dramatic reduction in appetite<sup>24</sup> and

undergo “test bouts” of shallow torpor,<sup>35</sup> while IBAs are brief periods of activity between two torpor bouts.

To determine changes in individual peptides throughout the year, we used univariate statistics to make pairwise comparisons for each temporally sequential transition: 1) August active to October; 2) October to December-January torpor; 3) December-January torpor to December-February IBA; 4) December-January torpor to March active; and 5) March active to August active (Figure 3). Consistent with the PCA, major changes were observed in the pairwise comparisons for the August active to October, December-January torpor to March active, and March active to August active transitions. Minimal or no significant peptide changes were observed for the October to December-January torpor or December-January torpor to December-February IBA transitions.

Transitioning from August to October, we saw a significant increase in peptides derived from CHGB, PENK, SCG2, SCG3, and SST, and a decrease in peptides derived from AVP, CHGB, PCSK1N (proSAAS), PCSK2, POMC, and SCG5 (Table 1). For the December-January Torpor to March active transition, we saw an overall increase in most detected peptides (Figure 3 and Supporting Document), including those from CHGB, PCSK1N (proSAAS), PENK, POMC, SCG3, SCG5, and SST. The general increase in abundance for many peptides immediately post-torpor is consistent with the physiology and behavior of the animal. During this transition, the animal shifts from a relatively inactive physiology to fully active, and thus may need a general increase in many pituitary peptide hormones to regulate a variety of processes. Finally, for the March to August transition, we saw increases in peptides from AVP, PCSK2, and several peptides from POMC, and a decrease in peptides from CHGB, CRH, GNRH1, PENK, SCG2, SCG3, SCG5, SST, and some peptides from POMC (Table 2). In addition to the pairwise comparisons of chronological time points, we also examined a pairwise comparison of the October to the March time points (Figure S7), as these are major seasonal transitions into and out of hibernation. Overall, March showed significantly higher levels of peptides from several prohormones, including CHGB, POMC, and PENK.

Overall, our results show significant changes in pituitary peptide hormones predominantly outside of the hibernation period. The lack of significant peptide changes for October to December-January torpor or for December-January torpor to December-February IBA transitions indicates that pituitary peptides may not play a major role in the immediate induction and regulation of the torpor state. Instead, the large changes in specific peptide hormones moving from August to October (pre-torpor), Torpor to March (post-torpor), and from March to August suggest that these hormones play roles in preparing the animal to enter and exit torpor (e.g., regulating metabolism and physiological extremes) rather than during torpor and IBA events.

### Dynamics of hypothalamus peptides

Hypothalamus peptides were identified from 45 animals (n = 8-11 per activity state). Immediately following database identification, 554 different peptides were identified with a 1% FDR. Following processing, 112 hypothalamus peptides were deemed “present” and appropriate for statistical analysis across samples (See Supporting Document). In

contrast to the pituitary, which was highly enriched in prohormone-derived peptides, the hypothalamus had a large number of endogenous peptides arising from non-prohormone proteins, such as hemoglobin, myelin basic protein, and others. This is consistent with previous peptidomic analysis of the hypothalamus.<sup>39</sup> Nevertheless, ~1/3 of the identified peptides were prohormone-derived, including from CHGB, PCSK1N (proSAAS), PDYN, PENK, TAC1, and others.

PCA of hypothalamus peptides showed clustering and clear separation for each activity state, with the greatest separation between the October group and the other groups (Figure 2 and Figure S8). Consistent with this observation, pairwise comparisons using univariate statistics showed greatest changes going into and out of October (Figure 4). Interestingly, we observed an overall increase in most detected prohormone-derived peptides in October relative to August and December-January torpor states, including peptides from CARTPT, CHGB, NPY, PCSK1N (proSAAS), PCSK2, PDYN, PENK, PMCH, TAC1, and TRH (Table 3). The general increase in many hypothalamic neuropeptides likely reflects a major activation of the hypothalamus during the transition to the winter months. Previous studies have suggested that the hypothalamus is a major regulator of hibernation, remains relatively active even during the torpid state, and may play a role in coordinating arousal signals.<sup>20, 41, 42</sup> Consistent with these observations, we observed significant changes in several hypothalamic neuropeptides for the December-January torpor to December-February IBA transition (Table 4). This includes an increase in endorphin peptides from PENK and PDYN, in addition to peptides from CARTPT, CHGB, TAC1, and TRH during periods of IBA. Overall, non-targeted peptidomic analysis of the hypothalamus revealed general prohormone-derived peptide increases in the pre-torpor October time point, general decreases as the animals enter torpor, and increases of a subset of neuropeptides during IBAs.

## Discussion

Throughout the year, hibernating mammals undergo major changes in physiology, but the molecular mechanisms underlying these changes, and how their tissues survive such physiological extremes, remain relatively unknown. Because cell-cell signaling peptides are known to play critical roles in mammalian physiology, we hypothesized that changes in endogenous peptide levels in the thirteen-lined ground squirrel central nervous system may correlate with the induction and maintenance of hibernation. To test this hypothesis, we performed non-targeted LC-MS and LC-MS/MS-based peptidomics analyses of the ground squirrel hypothalamus and pituitary. We found changes in several endogenous peptides throughout different time points in hibernation in both tissues. Some of these changes are consistent with prior hypotheses regarding specific peptides' roles in hibernation, while others are new observations.

Hibernation-relevant changes in physiology such as feeding behavior, energy balance, and body temperature are known in non-hibernating mammals to be partially regulated by peptides such as neuropeptide Y (from NPY),  $\alpha$ -MSH (from POMC), thyrotropin-releasing hormone (from TRH), and cocaine- and amphetamine-regulated transcript (from CARTPT).<sup>24, 43-47</sup> Our results reveal the dynamics of peptides from these prohormones



during hibernation, as well as from others which play roles in hibernation-relevant physiology (representative functions of some well-studied peptides are shown in Table S1). As one example, NPY has previously been shown to increase food intake and promote white adipose lipid storage, while decreasing metabolism and body temperature in rats.<sup>48-50</sup> In addition, exogenous administration of NPY has been shown to induce torpor-like reductions in body temperatures in Siberian hamsters.<sup>51</sup> Our results are consistent with these prior studies, and our observed increase in hypothalamic neuropeptide Y abundance in the August to October transition (Figure 5) may play a role in regulating food intake and decreasing energy expenditure as the animal prepares to enter the hibernation season.

Peptides from PCSK1N (proSAAS), including PEN, BigLEN, and LittleSAAS, were found to change in both the pituitary and the hypothalamus (Figure 5). ProSAAS peptides have been implicated in a number of physiological functions, including major roles in the regulation of feeding and body weight.<sup>52-55</sup> For example, exogenous microinjections of BigLEN into the nucleus accumbens of the rat brain were found to significantly increase food and water intake,<sup>52</sup> and intracerebroventricular injections of antibodies directed against BigLEN and PEN reduced food intake in fasted mice.<sup>53</sup> Our results showed an increase in proSAAS peptides (including BigLEN and PEN) in the hypothalamus during the August to October transition, and a decrease in these peptides as the animals transition into torpor. We also observed a decrease in proSAAS peptides in the pituitary during the August to October transition. During the Fall, thirteen-lined ground squirrels accumulate lipid in white adipose, after which satiety signals decrease overall food intake as the animals enter hibernation.<sup>24</sup> Changes in proSAAS peptide levels during this time period likely indicate that these peptides play a key role in pre-hibernation feeding and body weight regulation.

In addition to numerous peptides with direct roles in feeding and energy regulation, we also observed changes in many opioid peptides throughout hibernation. Opioid peptides play a wide variety of roles in physiology, including in pain perception and analgesia, reward response, stress response, and cardiovascular control.<sup>12, 56, 57</sup> We observed endogenous opioid peptides changing during hibernation, including enkephalins from PENK (Figure 5), neodynorphins from PDYN, and  $\beta$ -endorphins from POMC. In the pituitary, we observed a general decrease in specific opioid peptides as the animal entered the hibernation season (October), followed by a general increase as it exited hibernation (March). In the hypothalamus, we saw an increase in opioid peptides in October, followed by a decrease as the animal entered torpor. Perhaps most interestingly, we observed an increase in select hypothalamic opioid peptides (from both PENK and PDYN) during IBA relative to torpor, suggesting that these peptides may play important roles during these brief periods of activity during the hibernation season. These results are consistent with prior studies suggesting the involvement of opioid peptides and their receptors during hibernation and hibernation-like phenotypes<sup>28, 29, 58, 59</sup> and demonstrating that opioid peptides can reduce the duration of torpor bouts.<sup>60</sup> Importantly, delta opioid receptor agonists have been shown to provide neuroprotection against ischemia and reperfusion injury,<sup>61-64</sup> suggesting that the increase in endogenous opioid peptides during IBA may be playing a neuroprotective role during the dramatic change in physiology.

In addition to some of the examples given above, significant changes were also seen for peptides from prohormones such as CHGB, POMC, TAC1, AVP, SST, TRH, CARTPT, PMCH, and more. Many of these peptides do not have well-established functions, and our results suggest that these peptides may play roles in the hibernation process. For example, CHGB belongs to the granin family of proteins and plays important roles in prohormone processing and secretion.<sup>65</sup> In addition, the CHGB precursor protein itself is specifically processed into a number of peptides,<sup>66-68</sup> and the functions of most of these peptides are not known. Our analysis revealed many of these peptides are present and change throughout the hibernation cycle in both tissues. Similarly, peptides detected from CARTPT, TAC1, and TRH without well-studied functions were all seen to increase in the hypothalamus during IBA (Table 4). Our results directly identified the exact sequences of these peptides and quantified their changes during the stages of hibernation.

Several of the prohormone-derived peptides in the hypothalamus show significantly higher levels in both October (vs. August; Table 3) and IBA (vs. Torpor; Table 4) based on pairwise comparisons. Specifically, 13 of the 14 prohormone-derived peptides showing statistically higher levels during IBA are also elevated during October. These include six peptides derived from PENK, three from CHGB, and one each from CARTPT, TAC1, and TRH, as well as opioid peptides Met-enkephalin-Arg-Phe, Met-enkephalin-Arg-Gly-Leu, and  $\beta$ -neoendorphin. As noted above, opioid peptides and their receptors play important roles in pain, stress, and cardiovascular control, and have also been suggested to play a role in regulation and neuroprotection during hibernation. The function of most of the other peptides increasing during IBA are unknown, however elevated levels during both October and IBA may indicate their role in the transition between the active and torpid state. October marks the seasonal transition from summer activity to hibernation and therefore may account for the larger number of significantly changing prohormone-derived hypothalamus peptides compared to the 14 peptides elevated during the brief (< 24 h) IBA transitions that occur throughout hibernation.

Prior studies examining the transcriptomes of hibernators have revealed some insight into potential peptide changes during hibernation.<sup>24, 25</sup> However, transcriptomic analysis measures mRNA abundance, and cannot give information on translation into prohormones, processing of these prohormones into mature cell-cell signaling peptides, or degradation of these peptides after synthesis. Thus, the identity and abundance of the individual cell-cell signaling peptides cannot be inferred from transcriptomic information alone. This is especially true for hibernating animals, where dramatic reduction in core body temperature is expected to greatly reduce rates of macromolecular reactions such as translation, post-translational processing into mature cell-cell signaling peptides, and post-release degradation by endogenous proteases. Some of our results were consistent with prior transcriptome information.<sup>24, 25</sup> For example, transcriptomic analysis showed increases in hypothalamic TRH and CARTPT transcripts during the October transition, and our peptidomics measurements showed peptides from these prohormones also increased. In contrast, other results were not predictable from the transcriptome data, including the dynamics of neuropeptide Y, opioid peptides, and proSAAS-derived peptides during both October and IBA. These contrasts highlight the importance of direct peptide measurement that we have carried out here. In terms of measuring individual peptides, prior studies



have done so in a targeted manner (e.g., using immunoassays).<sup>27-29</sup> These methods require preselection of peptides of interest and often do not allow one to distinguish between modified forms of a given peptide. In contrast, LC-MS-based peptidomics does not require preselection of peptides and can accurately detect most PTMs, facilitating novel discoveries among a profile of detected peptides. Indeed, our analysis identified many unique peptides arising from any given precursor protein, allowing us to directly monitor changes in the signaling molecules themselves, including differentially processed forms of the same parent peptide sequence.

There are some important limitations to our study. First, while our results provide important insight into changes of endogenous peptides with season and activity state, we do not know the precise mechanism by which these peptides function with respect to hibernation. Examining the detailed roles of these identified peptides in the animal are important future goals. Second, while we attempted to keep dissection times as consistent as possible between animals, there was a minor difference in hypothalamus dissection times between different activity states, with the average time for August dissections taking ~30 s longer than other time points (see Figure S1). This small increase in dissection time may have led to more post-mortem proteolytic degradation for these samples relative to others. However, we did not see many significant differences in the March to August comparison (Figure 4), suggesting that this difference in dissection time did not have a major impact on peptide abundance. Third, because ground squirrels must be caught in the wild, we were unable to control the female:male ratio of animals in this study. The final ratio used for this study was disproportionately female, with a ~18:1 female:male ratio for the pituitary and a ~10:1 female:male ratio for the hypothalamus. As a result, the peptide changes we observed may be specific for female animals, and future studies may be necessary to tease apart sex differences. Finally, the methods we used for sample processing and database-based identifications are not compatible with some peptide sequences, particularly those that are very short or do not fragment well during MS/MS. As a result, we were not able to quantify some well-studied peptides such as thyrotropin-releasing hormone (pyroGlu-His-Pro-NH<sub>2</sub>), Met-enkephalin (Tyr-Gly-Gly-Phe-Met-OH), or the full-length CART peptide sequence. Nevertheless, our results provide valuable insight into many peptides that have not previously been implicated in the hibernation process.

In conclusion, our results are the first to apply non-targeted LC-MS and LC-MS/MS-based peptidomic measurements to study endogenous peptide dynamics during mammalian hibernation. Understanding cell-cell signaling is an important element in determining how natural hibernators survive physiological extremes that would be lethal to most mammals. Potential application of hibernation strategies to human medicine includes improvements in the preservation of organs used for transplantation, preventing debilitating reperfusion injury following myocardial infarction and stroke, improved treatment of trauma and hemorrhagic shock, and developing new strategies to combat obesity.<sup>2, 4</sup> Our work sets the stage for a number of follow-up studies to examine the roles of specific endogenous peptides in hibernation, with the long-term goal of applying these strategies to benefit human health.

## Methods

### Materials

Unless otherwise specified, all solvents and reagents were purchased from ThermoFisher Scientific or MilliporeSigma.

### Animals and tissue collection

All animal experiments and procedures were completed in accordance with protocols approved by the Institutional Animal Care and Use Committee of the University of Nebraska-Lincoln (Project ID 1927) and performed according to the Guide for the Care and Use of Laboratory Animals. Thirteen-lined ground squirrels (*Ictidomys tridecemlineatus*) used in this study were captured in the vicinity of Lincoln, Nebraska during the summer months and transported to the veterinary facilities of the UNL Institutional Animal Care Program. During the “active” season (March–October), animals were housed individually in standard rodent cages under 12:12 h light:dark cycle, ambient temperature of ~20 °C, with water and food (rodent chow ad libitum and sunflower seeds). During the hibernation season (November–February) squirrels were housed in an environmental chamber with constant conditions (water available, no food provided, 24 hours of darkness, and ambient temperature of 5 °C).

On the day of necropsy, the animal was removed from its cage, body weight was recorded, and the animal was sacrificed by rapid decapitation. The body temperature of animals in the “October”, “torpor”, and “IBA” groups were measured by rectal thermometer immediately after decapitation. Following decapitation, the hypothalamus and pituitary were dissected, immediately placed in cryogenic vials, and flash-frozen in liquid nitrogen. Gross boundaries of the hypothalamus include the optic chiasm and rostral commissure rostrally, cerebral crura laterally, interpeduncular fossa caudally, and thalamus dorsally. The pituitary stalk was separated upon brain removal. Thus, the pituitary gland was collected from the hypophyseal fossa of the sphenoid bone. Frozen tissues were stored on dry ice after flash freezing, and then moved to –80 °C until peptide extraction. Peptides were extracted from tissues on the same day as necropsy.

For the pituitary, n = 37 animals were analyzed from August (n = 9), October (n = 9), torpor (n = 5), IBA (n = 6), and March (n = 8). For the hypothalamus, n = 45 animals were analyzed from August (n = 9), October (n = 9), torpor (n = 11), IBA (n = 8), and March (n = 8). Although we aimed to have roughly equal sample sizes between tissues for each group, tissues from some animals could not be isolated and others gave total peptide yields below that which is necessary for LC-MS analysis.

### Peptide extraction and sample preparation

Tissues were transferred to microcentrifuge tubes and homogenized using plastic pestles (Bel-Art, BEL-19923-0001) in 400 µL of ice-cold acidified acetone (acetone:H<sub>2</sub>O:HCl = 40:6:1, v/v/v), briefly vortexed, sonicated for 5 min, and centrifuged (15,000 × g, 10 min, 4 °C). Following centrifugation, the supernatant was carefully transferred to clean microcentrifuge tubes and stored on ice, and the pellet was subjected to a second stage of

extraction using 400  $\mu\text{L}$  ice-cold acidified water (0.25% (v/v) acetic acid in water) using the same procedure as the first stage. Following centrifugation, the supernatants from both stages were combined and solvent removed via vacuum concentrator. The resulting dried extracts were resuspended in 300  $\mu\text{L}$  of 5% acetonitrile (ACN)/ $\text{H}_2\text{O}$  + 0.1% formic acid (FA), sonicated for 3 min, and centrifuged (15,000  $\times$  g, 10 min, 4  $^\circ\text{C}$ ). The supernatant was removed and passed through a pre-rinsed 30 kDa molecular weight filtration device (MilliporeSigma, UFC503024) to remove high molecular weight species (14,000  $\times$  g, ~15 min, 4  $^\circ\text{C}$ ). To ensure maximum recovery, 200  $\mu\text{L}$  of 5% ACN/ $\text{H}_2\text{O}$  + 0.1% FA was added to the filtration device and centrifuged, and this was repeated for a total of two rinses. The collected filtrate was then dried via vacuum concentrator. Dried peptide extracts were dissolved in 200  $\mu\text{L}$  of 5% ACN/ $\text{H}_2\text{O}$  + 0.1% FA and then desalted by using a C18 spin column (ThermoFisher Scientific, 89873). Eluted desalted peptide extracts were dried via vacuum concentrator and stored at  $-20^\circ\text{C}$  until LC-MS and LC-MS/MS analysis.

### LC-MS and LC-MS/MS analysis

LC-MS and LC-MS/MS analysis was performed on peptide samples after all tissues had been collected and peptides extracted. Desalted peptide extracts were dissolved in 12  $\mu\text{L}$  of 3% ACN/ $\text{H}_2\text{O}$  + 0.1% FA. 2  $\mu\text{L}$  of this redissolved extract were removed and used to determine the total protein concentration by BCA protein assay (Micro BCA Protein Assay Kit, Thermo Scientific, 23235). Each sample was then diluted to allow sample injections of 300 ng total protein for hypothalamus or 200 ng total protein for pituitary. For each tissue, a pooled QC sample was created by mixing an equal volume of each sample.

Within each tissue, samples were analyzed by LC-MS and LC-MS/MS in a randomized injection order with regular injections of pooled QC sample. LC-MS and LC-MS/MS analysis was performed on a Waters G2-SX Q-ToF mass spectrometer equipped with a Waters UPLC M-Class system with reversed-phase separation and a Waters NanoESI source (Zspray, NanoLockSpray). For reversed-phase separation, Solvent A contained  $\text{H}_2\text{O}$  + 0.1% FA and Solvent B contained ACN + 0.1% FA. After sample injection, samples were loaded onto a Waters C18 trap column (180  $\mu\text{m}$   $\times$  20 mm, 186008821) at a flow rate of 5  $\mu\text{L}/\text{min}$  and 1% Solvent B for 10 min. Peptide separation was carried out over 60 min with a 0.35  $\mu\text{L}/\text{min}$  flow rate and 35  $^\circ\text{C}$  column temperature using a Waters nanoEase-C18 column (75  $\mu\text{m}$   $\times$  250 mm, 186008818). The gradient for separation was as follows: 0 – 40 min, 3 – 40% B; 40 – 44 min, 40 – 85% B; 44 – 48 min, 85% B; 48 – 50 min, 85 – 3% B; 50 – 60 min, 3% B. MS/MS was performed by collision-induced dissociation (CID) using the following settings: mass range, 100–2000 m/z; 3 precursor ions, peak intensity threshold of 5000, the MS scan time was 0.1 s, MS/MS scan time was 0.5 s, and in collision energy ramp mode.

### Data processing and statistical analysis

Peptide identifications were made using PEAKS Studio X Pro (Bioinformatics Solutions Inc.),<sup>69, 70</sup> searching against the *Ictidomys tridecemlineatus* proteome database available from Uniprot.<sup>71</sup> Peptide identifications were conducted using the following parameters: parent mass error tolerance was set to 10 ppm, fragment mass error tolerance was set to 0.1 Da, and the following PTMs were considered: oxidation (M), amidation, acetylation, pyroglutamylation (Q or E), and phosphorylation (S, T, or Y). A 1% false discovery

rate (FDR) threshold was used for peptide identifications. Label-free quantification was performed with the PEAKS Q Module, which helps to reduce missing values using ID-transfer and calculates peptide peak areas. For the Q Module, a mass error tolerance of 20.0 ppm and a retention time shift tolerance of 2.5 minutes were used. Peptide peak intensities were normalized to the total ion current (TIC) and exported from the Q Module for further analysis. During ID-transfer, distinct peptides with close  $m/z$  and retention times may be assigned to the same peak in the absence of MS/MS spectra. In such cases, the identity of the given peptide is ambiguous and not reliable for making comparisons. Peptide peaks with ambiguous assignments or peptides with <5 total MS/MS identifications were filtered out during this preprocessing step.

Data were batch corrected using the statTarget R package,<sup>72</sup> where a peptide was considered present if it was measured in at least 50% of the samples per group. Peptides deemed absent were omitted after batch correction, leaving 94 peptides “present” in pituitary and 112 peptides “present” in hypothalamus and appropriate for statistical analysis. Signal imputation were performed using k-nearest neighbor (knn; k=10).<sup>73</sup> Present peptides underwent a log<sub>2</sub> transformation and were normalized using EigenMS.<sup>74, 75</sup> Data preprocessing was prepared using the R statistical software version 4.2.1.<sup>76</sup>

Differentially abundant peptides were assessed using parametric (t-test) and non-parametric (Wilcoxon rank-sum) statistical tests to account for the degree, direction, and difference between each pair of time points within each tissue. For both statistical tests, the Benjamini-Hochberg (BH) procedure was applied to correct for multiple hypothesis testing.<sup>77</sup> Peptides were considered differentially abundant when they passed with a BH corrected p-value less than 0.05 in both statistical tests. The fold change (FC) was calculated for each peptide to quantify the magnitude difference between each pair of time points. Principal component analysis (PCA) was performed using R package pcaMethods.<sup>78</sup>

The mass spectrometry peptidomics data have been deposited to the ProteomeXchange Consortium via the PRIDE<sup>79</sup> partner repository with the dataset identifier PXD040033 and 10.6019/PXD040033.

## Supplementary Material

Refer to Web version on PubMed Central for supplementary material.

## Acknowledgments

This research was supported by the National Institute of General Medical Sciences (R35 GM142784 to J.W.C.). We also acknowledge support from the Nebraska Center for Integrated Biomolecular Communication (NCIBC, National Institute of General Medical Sciences P20 GM113126). We thank Frazer I. Heimis, Eric Tom, and Md Shadman Ridwan Abid for their help with animal procedures. We are grateful for the assistance provided by the University of Nebraska-Lincoln Institutional Animal Care Program and the staff of Life Sciences Annex for oversight of animal protocols, training and experimental assistance, and additional resources. Finally, we thank the Nebraska Center for Mass Spectrometry, NCIBC Systems Biology Core Facility, and the Research Instrumentation Facility for providing instrument access.

## References

1. Carey HV, Andrews MT, and Martin SL (2003) Mammalian hibernation: cellular and molecular responses to depressed metabolism and low temperature, *Physiol. Rev* 83, 1153–1181. [PubMed: 14506303]
2. Andrews MT (2019) Molecular interactions underpinning the phenotype of hibernation in mammals, *J. Exp. Biol* 222, jeb160606. [PubMed: 30683731]
3. Mohr SM, Bagriantsev SN, and Gracheva EO (2020) Cellular, Molecular, and Physiological Adaptations of Hibernation: The Solution to Environmental Challenges, *Annu. Rev. Cell Dev. Biol* 36, 315–338. [PubMed: 32897760]
4. Drew KL, Buck CL, Barnes BM, Christian SL, Rasley BT, and Harris MB (2007) Central nervous system regulation of mammalian hibernation: implications for metabolic suppression and ischemia tolerance, *J. Neurochem* 102, 1713–1726. [PubMed: 17555547]
5. Wolf A, Mulier KE, Muratore SL, and Beilman GJ (2017) D-beta-Hydroxybutyrate and melatonin for treatment of porcine hemorrhagic shock and injury: a melatonin dose-ranging study, *BMC Res. Notes* 10, 649. [PubMed: 29187245]
6. Klein AH, Wendroth SM, Drewes LR, and Andrews MT (2010) Small-volume d-beta-hydroxybutyrate solution infusion increases survivability of lethal hemorrhagic shock in rats, *Shock* 34, 565–572. [PubMed: 20386494]
7. Perez de Lara Rodriguez CE, Drewes LR, and Andrews MT (2017) Hibernation-based blood loss therapy increases survivability of lethal hemorrhagic shock in rats, *J. Comp. Physiol. B* 187, 769–778. [PubMed: 28324159]
8. Nillni EA, Xie W, Mulcahy L, Sanchez VC, and Wetsel WC (2002) Deficiencies in pro-thyrotropin-releasing hormone processing and abnormalities in thermoregulation in *Cpe<sup>fat/fat</sup>* mice, *J. Biol. Chem* 277, 48587–48595. [PubMed: 12270926]
9. Szentirmai E, Kapas L, Sun Y, Smith RG, and Krueger JM (2009) The preproghrelin gene is required for the normal integration of thermoregulation and sleep in mice, *Proc. Natl. Acad. Sci. U. S. A* 106, 14069–14074. [PubMed: 19666521]
10. Morton GJ, Cummings DE, Baskin DG, Barsh GS, and Schwartz MW (2006) Central nervous system control of food intake and body weight, *Nature* 443, 289–295. [PubMed: 16988703]
11. Atkins N Jr., Ren S, Hatcher N, Burgoon PW, Mitchell JW, Sweedler JV, and Gillette MU (2018) Functional peptidomics: stimulus- and time-of-day-specific peptide release in the mammalian circadian clock, *ACS Chem. Neurosci* 9, 2001–2008. [PubMed: 29901982]
12. Fricker LD, Margolis EB, Gomes I, and Devi LA (2020) Five decades of research on opioid peptides: current knowledge and unanswered questions, *Mol. Pharmacol* 98, 96–108. [PubMed: 32487735]
13. Hokfelt T, Bartfai T, and Bloom F (2003) Neuropeptides: opportunities for drug discovery, *Lancet Neurol.* 2, 463–472. [PubMed: 12878434]
14. Hook V, Funkelstein L, Lu D, Bark S, Wegrzyn J, and Hwang SR (2008) Proteases for processing proneuropeptides into peptide neurotransmitters and hormones, *Annu. Rev. Pharmacol. Toxicol* 48, 393–423. [PubMed: 18184105]
15. Hook V, Lietz CB, Podvin S, Cajka T, and Fiehn O (2018) Diversity of neuropeptide cell-cell signaling molecules generated by proteolytic processing revealed by neuropeptidomics mass spectrometry, *J. Am. Soc. Mass. Spectrom* 29, 807–816. [PubMed: 29667161]
16. Fricker LD, Evans CJ, Esch FS, and Herbert E (1986) Cloning and sequence analysis of cDNA for bovine carboxypeptidase E, *Nature* 323, 461–464. [PubMed: 3020433]
17. Boonstra R, Bradley AJ, and Delehanty B (2011) Preparing for hibernation in ground squirrels: adrenal androgen production in summer linked to environmental severity in winter, *Funct. Ecol* 25, 1348–1359.
18. Frare C, Jenkins ME, Soldin SJ, and Drew KL (2018) The Raphe Pallidus and the Hypothalamic-Pituitary-Thyroid Axis Gate Seasonal Changes in Thermoregulation in the Hibernating Arctic Ground Squirrel (*Urocitellus parryii*), *Front. Physiol* 9, 1747. [PubMed: 30618783]
19. Frare C, Williams CT, and Drew KL (2021) Thermoregulation in hibernating mammals: The role of the "thyroid hormones system", *Mol. Cell. Endocrinol* 519, 111054. [PubMed: 33035626]

20. Junkins MS, Bagriantsev SN, and Gracheva EO (2022) Towards understanding the neural origins of hibernation, *J. Exp. Biol* 225, jeb229542. [PubMed: 34982152]
21. Takahashi TM, Sunagawa GA, Soya S, Abe M, Sakurai K, Ishikawa K, Yanagisawa M, Hama H, Hasegawa E, Miyawaki A, Sakimura K, Takahashi M, and Sakurai T (2020) A discrete neuronal circuit induces a hibernation-like state in rodents, *Nature* 583, 109–114. [PubMed: 32528181]
22. Hrvatin S, Sun S, Wilcox OF, Yao H, Lavin-Peter AJ, Cicconet M, Assad EG, Palmer ME, Aronson S, Banks AS, Griffith EC, and Greenberg ME (2020) Neurons that regulate mouse torpor, *Nature* 583, 115–121. [PubMed: 32528180]
23. Helwig M, Archer ZA, Heldmaier G, Tups A, Mercer JG, and Klingenspor M (2009) Photoperiodic regulation of satiety mediating neuropeptides in the brainstem of the seasonal Siberian hamster (*Phodopus sungorus*), *J. Comp. Physiol. A* 195, 631–642.
24. Schwartz C, Hampton M, and Andrews MT (2015) Hypothalamic gene expression underlying pre-hibernation satiety, *Genes Brain Behav.* 14, 310–318. [PubMed: 25640202]
25. Schwartz C, Hampton M, and Andrews MT (2013) Seasonal and regional differences in gene expression in the brain of a hibernating mammal, *PLoS One* 8, e58427. [PubMed: 23526982]
26. El Ouezani S, Lafon P, Tramu G, and Magoul R (2001) Neuropeptide Y gene expression in the jerboa arcuate nucleus: modulation by food deprivation and relationship with hibernation, *Neurosci. Lett* 305, 127–130. [PubMed: 11376900]
27. Gardi J, Nelson OL, Robbins CT, Szentirmai E, Kapas L, and Krueger JM (2011) Energy homeostasis regulatory peptides in hibernating grizzly bears, *Gen. Comp. Endocrinol* 172, 181–183. [PubMed: 21187098]
28. Bourhim N, Kabine M, and Elkebbaj MS (1997) Characterization of opioid peptides and opioid receptors in the brain of jerboa (*Jaculus orientalis*), a hibernating rodent, *Brain Res. Bull* 44, 615–620. [PubMed: 9365806]
29. Cui Y, Lee TF, and Wang LC (1996) State-dependent changes of brain endogenous opioids in mammalian hibernation, *Brain Res. Bull* 40, 129–133. [PubMed: 8724431]
30. Nürnberger F (1995) The neuroendocrine system in hibernating mammals: present knowledge and open questions, *Cell Tissue Res.* 281, 391–412. [PubMed: 7553762]
31. Fricker LD, Lim J, Pan H, and Che FY (2006) Peptidomics: identification and quantification of endogenous peptides in neuroendocrine tissues, *Mass Spectrom. Rev* 25, 327–344. [PubMed: 16404746]
32. Romanova EV, and Sweedler JV (2015) Peptidomics for the discovery and characterization of neuropeptides and hormones, *Trends Pharmacol. Sci* 36, 579–586. [PubMed: 26143240]
33. Abid MSR, Qiu H, Tripp BA, de Lima Leite A, Roth HE, Adamec J, Powers R, and Checco JW (2022) Peptidomics analysis reveals changes in small urinary peptides in patients with interstitial cystitis/bladder pain syndrome, *Sci. Rep* 12, 8289. [PubMed: 35585122]
34. Mousavi S, Qiu H, Heinis FI, Abid MSR, Andrews MT, and Checco JW (2022) Short-term administration of common anesthetics does not dramatically change the endogenous peptide profile in the rat pituitary, *ACS Chem. Neurosci* 13, 2888–2896. [PubMed: 36126283]
35. Russell RL, O'Neill PH, Epperson LE, and Martin SL (2010) Extensive use of torpor in 13-lined ground squirrels in the fall prior to cold exposure, *J. Comp. Physiol. B* 180, 1165–1172. [PubMed: 20556614]
36. Che FY, Lim J, Pan H, Biswas R, and Fricker LD (2005) Quantitative neuropeptidomics of microwave-irradiated mouse brain and pituitary, *Mol. Cell. Proteomics* 4, 1391–1405. [PubMed: 15970582]
37. Che FY, Yan L, Li H, Mzhavia N, Devi LA, and Fricker LD (2001) Identification of peptides from brain and pituitary of *Cpe<sup>fat</sup>/Cpe<sup>fat</sup>* mice, *Proc. Natl. Acad. Sci. U. S. A* 98, 9971–9976. [PubMed: 11481435]
38. Che FY, Yuan Q, Kalinina E, and Fricker LD (2005) Peptidomics of *Cpe fat/fat* mouse hypothalamus: effect of food deprivation and exercise on peptide levels, *J. Biol. Chem* 280, 4451–4461. [PubMed: 15572367]
39. Secher A, Kelstrup CD, Conde-Frieboes KW, Pyke C, Raun K, Wulff BS, and Olsen JV (2016) Analytic framework for peptidomics applied to large-scale neuropeptide identification, *Nat. Commun* 7, 11436. [PubMed: 27142507]



40. Che FY, and Fricker LD (2002) Quantitation of neuropeptides in Cpe(fat)/Cpe(fat) mice using differential isotopic tags and mass spectrometry, *Anal. Chem* 74, 3190–3198. [PubMed: 12141682]
41. Bratincsák A, McMullen D, Miyake S, Tóth ZE, Hallenbeck JM, and Palkovits M (2007) Spatial and temporal activation of brain regions in hibernation: c-fos expression during the hibernation bout in thirteen-lined ground squirrel, *J. Comp. Neurol* 505, 443–458. [PubMed: 17912746]
42. O'Hara BF, Watson FL, Srere HK, Kumar H, Wiler SW, Welch SK, Bitting L, Heller HC, and Kilduff TS (1999) Gene expression in the brain across the hibernation cycle, *J. Neurosci* 19, 3781–3790. [PubMed: 10234010]
43. Schwartz MW, Woods SC, Porte D Jr., Seeley RJ, and Baskin DG (2000) Central nervous system control of food intake, *Nature* 404, 661–671. [PubMed: 10766253]
44. Spiegelman BM, and Flier JS (2001) Obesity and the regulation of energy balance, *Cell* 104, 531–543. [PubMed: 11239410]
45. Ong ZY, and McNally GP (2020) CART in energy balance and drug addiction: Current insights and mechanisms, *Brain Res.* 1740, 146852. [PubMed: 32335093]
46. Baldini G, and Phelan KD (2019) The melanocortin pathway and control of appetite-progress and therapeutic implications, *J. Endocrinol* 241, R1–r33. [PubMed: 30812013]
47. Zhang W, Cline MA, and Gilbert ER (2014) Hypothalamus-adipose tissue crosstalk: neuropeptide Y and the regulation of energy metabolism, *Nutr. Metab* 11, 27.
48. Bouali SM, Fournier A, St-Pierre S, and Jolicœur FB (1995) Influence of ambient temperature on the effects of NPY on body temperature and food intake, *Pharmacol. Biochem. Behav* 50, 473–475. [PubMed: 7617688]
49. Billington CJ, Briggs JE, Grace M, and Levine AS (1991) Effects of intracerebroventricular injection of neuropeptide Y on energy metabolism, *Am. J. Physiol* 260, R321–327. [PubMed: 1996719]
50. Egawa M, Yoshimatsu H, and Bray GA (1991) Neuropeptide Y suppresses sympathetic activity to interscapular brown adipose tissue in rats, *Am. J. Physiol* 260, R328–334. [PubMed: 1996720]
51. Paul MJ, Freeman DA, Park JH, and Dark J (2005) Neuropeptide Y induces torpor-like hypothermia in Siberian hamsters, *Brain Res.* 1055, 83–92. [PubMed: 16098953]
52. Ye H, Wang J, Tian Z, Ma F, Dowell J, Bremer Q, Lu G, Baldo B, and Li L (2017) Quantitative mass spectrometry reveals food intake-induced neuropeptide level changes in rat brain: functional assessment of selected neuropeptides as feeding regulators, *Mol. Cell. Proteomics* 16, 1922–1937. [PubMed: 28864778]
53. Wardman JH, Berezniuk I, Di S, Tasker JG, and Fricker LD (2011) ProSAAS-derived peptides are colocalized with neuropeptide Y and function as neuropeptides in the regulation of food intake, *PLoS One* 6, e28152. [PubMed: 22164236]
54. Gomes I, Aryal DK, Wardman JH, Gupta A, Gagnidze K, Rodriguiz RM, Kumar S, Wetsel WC, Pintar JE, Fricker LD, and Devi LA (2013) GPR171 is a hypothalamic G protein-coupled receptor for BigLEN, a neuropeptide involved in feeding, *Proc. Natl. Acad. Sci. U. S. A* 110, 16211–16216. [PubMed: 24043826]
55. Wei S, Feng Y, Che FY, Pan H, Mzhavia N, Devi LA, McKinzie AA, Levin N, Richards WG, and Fricker LD (2004) Obesity and diabetes in transgenic mice expressing proSAAS, *J. Endocrinol* 180, 357–368. [PubMed: 15012590]
56. Akil H, Watson SJ, Young E, Lewis ME, Khachaturian H, and Walker JM (1984) Endogenous opioids: biology and function, *Annu. Rev. Neurosci* 7, 223–255. [PubMed: 6324644]
57. Feng Y, He X, Yang Y, Chao D, Lazarus LH, and Xia Y (2012) Current research on opioid receptor function, *Curr Drug Targets* 13, 230–246. [PubMed: 22204322]
58. Tamura Y, Shintani M, Nakamura A, Monden M, and Shiomi H (2005) Phase-specific central regulatory systems of hibernation in Syrian hamsters, *Brain Res.* 1045, 88–96. [PubMed: 15910766]
59. Cintron-Colon R, Johnson CW, Montenegro-Burke JR, Guijas C, Faulhaber L, Sanchez-Alavez M, Aguirre CA, Shankar K, Singh M, Galmozzi A, Siuzdak G, Saez E, and Conti B (2019) Activation of Kappa Opioid Receptor Regulates the Hypothermic Response to Calorie Restriction and Limits Body Weight Loss, *Curr. Biol* 29, 4291–4299. [PubMed: 31786059]

60. Beckman AL, Lladós-Eckman C, and Stanton TL (1992) Reduction of hibernation bout duration by intraventricular infusion of met-enkephalin, *Brain Res.* 588, 159–163. [PubMed: 1393565]
61. Yang Y, Xia X, Zhang Y, Wang Q, Li L, Luo G, and Xia Y (2009) delta-Opioid receptor activation attenuates oxidative injury in the ischemic rat brain, *BMC Biol.* 7, 55. [PubMed: 19709398]
62. Borlongan CV, Hayashi T, Oeltgen PR, Su TP, and Wang Y (2009) Hibernation-like state induced by an opioid peptide protects against experimental stroke, *BMC Biol.* 7, 31. [PubMed: 19534760]
63. Gao CJ, Li JP, Wang W, Lü BC, Niu L, Zhu C, Wei YY, Zhang T, Wu SX, Chai W, and Li YQ (2010) Effects of intracerebroventricular application of the delta opioid receptor agonist [D-Ala<sup>2</sup>, D-Leu<sup>5</sup>] enkephalin on neurological recovery following asphyxial cardiac arrest in rats, *Neuroscience* 168, 531–542. [PubMed: 20167252]
64. Chen M, Wu S, Shen B, Fan Q, Zhang R, Zhou Y, Zhang P, Wang L, and Zhang L (2021) Activation of the  $\delta$  opioid receptor relieves cerebral ischemic injury in rats via EGFR transactivation, *Life Sci.* 273, 119292. [PubMed: 33667516]
65. Natori S, and Huttner WB (1996) Chromogranin B (secretogranin I) promotes sorting to the regulated secretory pathway of processing intermediates derived from a peptide hormone precursor, *Proc. Natl. Acad. Sci. U. S. A* 93, 4431–4436. [PubMed: 8633084]
66. Troger J, Theurl M, Kirchmair R, Pasqua T, Tota B, Angelone T, Cerra MC, Nowosielski Y, Mätzler R, Troger J, Gayen JR, Trudeau V, Corti A, and Helle KB (2017) Granin-derived peptides, *Prog. Neurobiol* 154, 37–61. [PubMed: 28442394]
67. Bartolomucci A, Possenti R, Mahata SK, Fischer-Colbrie R, Loh YP, and Salton SR (2011) The extended granin family: structure, function, and biomedical implications, *Endocr. Rev* 32, 755–797. [PubMed: 21862681]
68. Lee JC, and Hook V (2009) Proteolytic fragments of chromogranins A and B represent major soluble components of chromaffin granules, illustrated by two-dimensional proteomics with NH(2)-terminal Edman peptide sequencing and MALDI-TOF MS, *Biochemistry* 48, 5254–5262. [PubMed: 19405523]
69. Ma B, Zhang K, Hendrie C, Liang C, Li M, Doherty-Kirby A, and Lajoie G (2003) PEAKS: powerful software for peptide de novo sequencing by tandem mass spectrometry, *Rapid Commun. Mass Spectrom* 17, 2337–2342. [PubMed: 14558135]
70. Zhang J, Xin L, Shan B, Chen W, Xie M, Yuen D, Zhang W, Zhang Z, Lajoie GA, and Ma B (2012) PEAKS DB: de novo sequencing assisted database search for sensitive and accurate peptide identification, *Mol. Cell. Proteomics* 11, M111.010587.
71. UniProt Consortium. (2021) UniProt: the universal protein knowledgebase in 2021, *Nucleic Acids Res.* 49, D480–D489. [PubMed: 33237286]
72. Luan H, Ji F, Chen Y, and Cai Z (2018) starTarget: A streamlined tool for signal drift correction and interpretations of quantitative mass spectrometry-based omics data, *Anal. Chim. Acta* 1036, 66–72. [PubMed: 30253838]
73. Cover T, and Hart P (1967) Nearest neighbor pattern classification, *IEEE Trans. Inf. Theory*, 21–27.
74. Karpievitch YV, Taverner T, Adkins JN, Callister SJ, Anderson GA, Smith RD, and Dabney AR (2009) Normalization of peak intensities in bottom-up MS-based proteomics using singular value decomposition, *Bioinformatics* 25, 2573–2580. [PubMed: 19602524]
75. Karpievitch YV, Stuart T, and Mohamed S (2021) ProteoMM: multi-dataset model-based differential expression proteomics analysis platform, R package version 1.12.0
76. RCoreTeam. (2022) R: A language and environment for statistical computing. R Foundation for Statistical Computing, Vienna, Austria. <https://www.r-project.org/>.
77. Benjamini Y, and Hochberg Y (1995) Controlling the false discovery rate: A practical and powerful approach to multiple testing, *J. R. Stat. Soc. Series B* 57, 289–300.
78. Stacklies W, Redestig H, Scholz M, Walther D, and Selbig J (2007) pcaMethods--a bioconductor package providing PCA methods for incomplete data, *Bioinformatics* 23, 1164–1167. [PubMed: 17344241]
79. Perez-Riverol Y, Bai J, Bandla C, García-Seisdedos D, Hewapathirana S, Kamatchinathan S, Kundu DJ, Prakash A, Frericks-Zipper A, Eisenacher M, Walzer M, Wang S, Brazma A, and

Vizcaíno JA (2022) The PRIDE database resources in 2022: a hub for mass spectrometry-based proteomics evidences, *Nucleic Acids Res.* 50, D543–d552. [PubMed: 34723319]

Author Manuscript

Author Manuscript

Author Manuscript

Author Manuscript

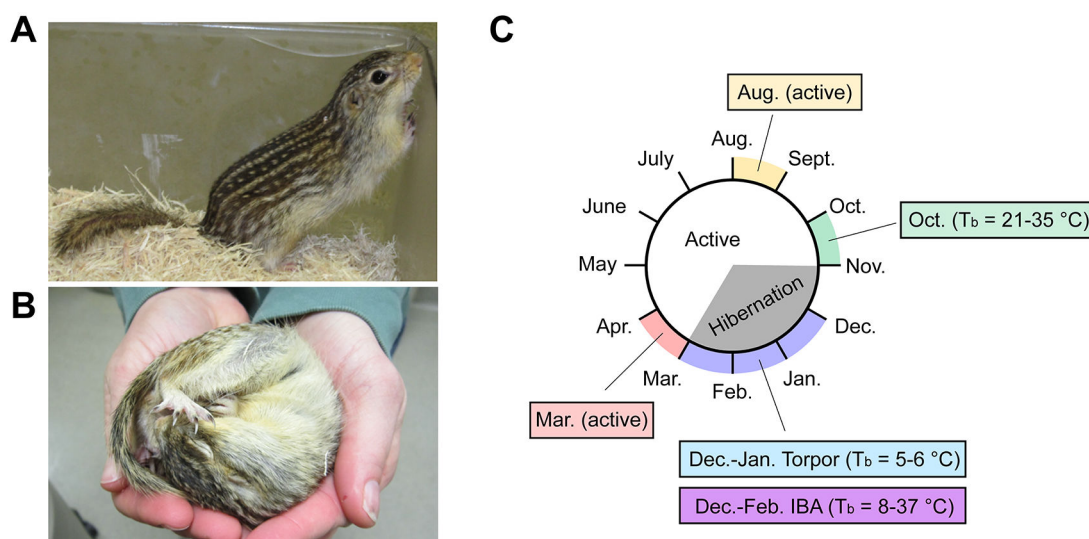


**Figure 1.**

The thirteen-lined ground squirrel hibernation cycle. (A) Active thirteen-lined ground squirrel. (B) Torpid thirteen-lined ground squirrel. (C) Overview of annual hibernation cycle and timeline for tissue sampling. The central circle represents months of the year progressing clockwise, with general active period in white, and the hibernation states of torpor and interbout arousal (IBA) in gray, as indicated in the center. Colored outer regions and text boxes indicate time points for sample collection for this study. For time points in pre-hibernation and hibernation season, the measured range of internal body temperatures is indicated in parentheses.

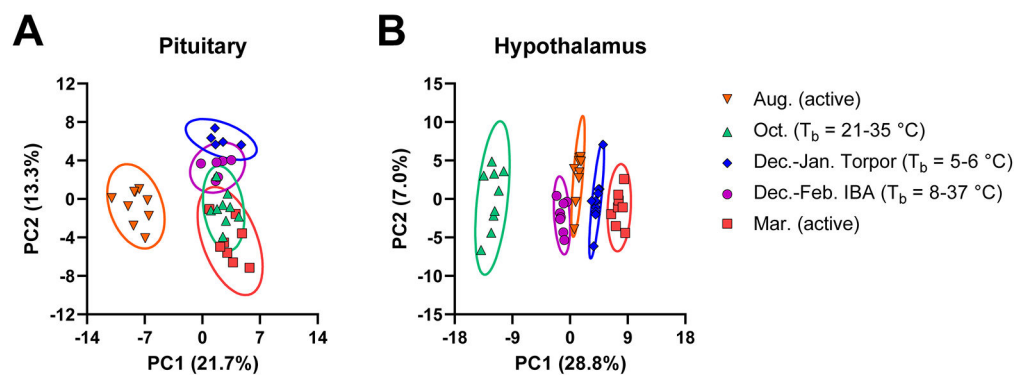


**Figure 2.**

Principle component analysis for LC-MS-measured peptide profile. PCA scores plots from the (A) pituitary and (B) hypothalamus after preprocessing and normalization by EigenMS. For the pituitary,  $n = 37$  animals were analyzed from August (Aug.,  $n = 9$ ), October (Oct.,  $n = 9$ ), torpor (Dec.-Jan. Torpor,  $n = 5$ ), IBA (Dec.-Feb. IBA,  $n = 6$ ), and March (Mar.,  $n = 8$ ). For the hypothalamus,  $n = 45$  animals were analyzed from August (Aug.,  $n = 9$ ), October (Oct.,  $n = 9$ ), torpor (Dec.-Jan. Torpor,  $n = 11$ ), IBA (Dec.-Feb. IBA,  $n = 8$ ), and March (Mar.,  $n = 8$ ).

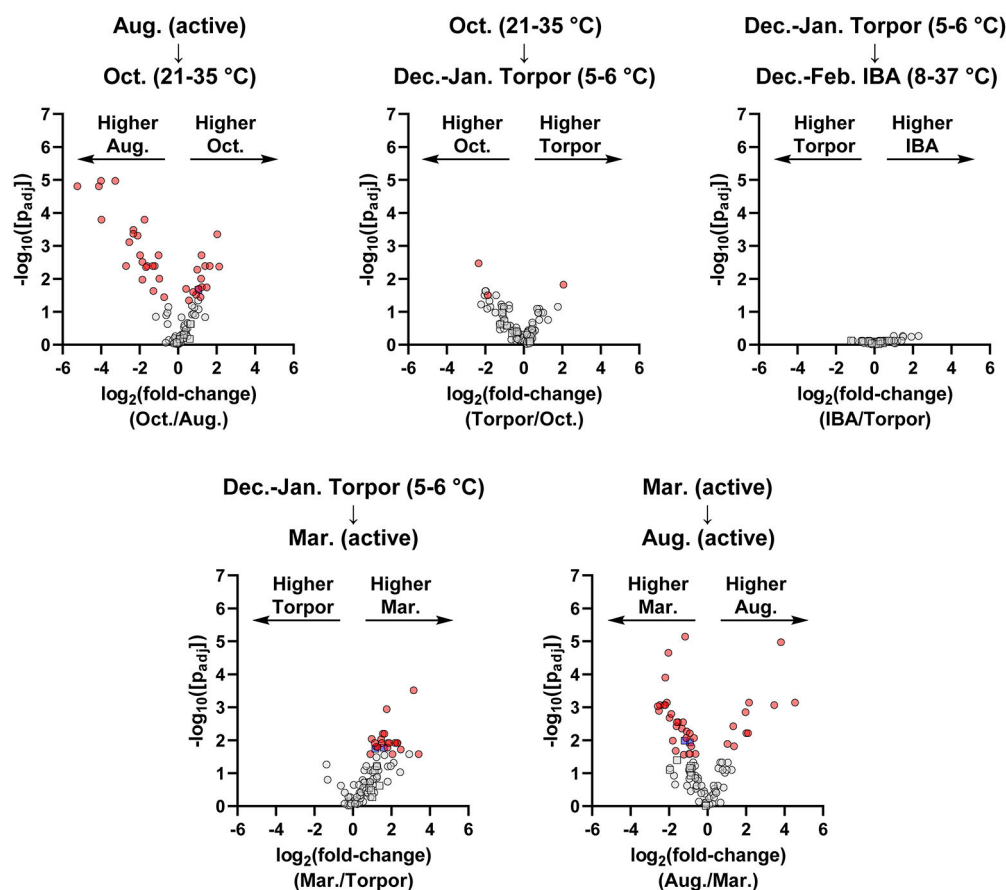


**Figure 3.**

Volcano plots representing pairwise comparisons for pituitary peptides for chronological transitions throughout the year. Circles represent prohormone-derived peptides, while squares indicate peptides arising from non-prohormone proteins. Red data points indicate significantly changing prohormone-derived peptides (passing both parametric and non-parametric tests with  $p < 0.05$ ). Blue data points indicate significantly changing non-prohormone derived peptides. Grey data points indicate peptides that were not significantly changing ( $p > 0.05$  in either or both tests).



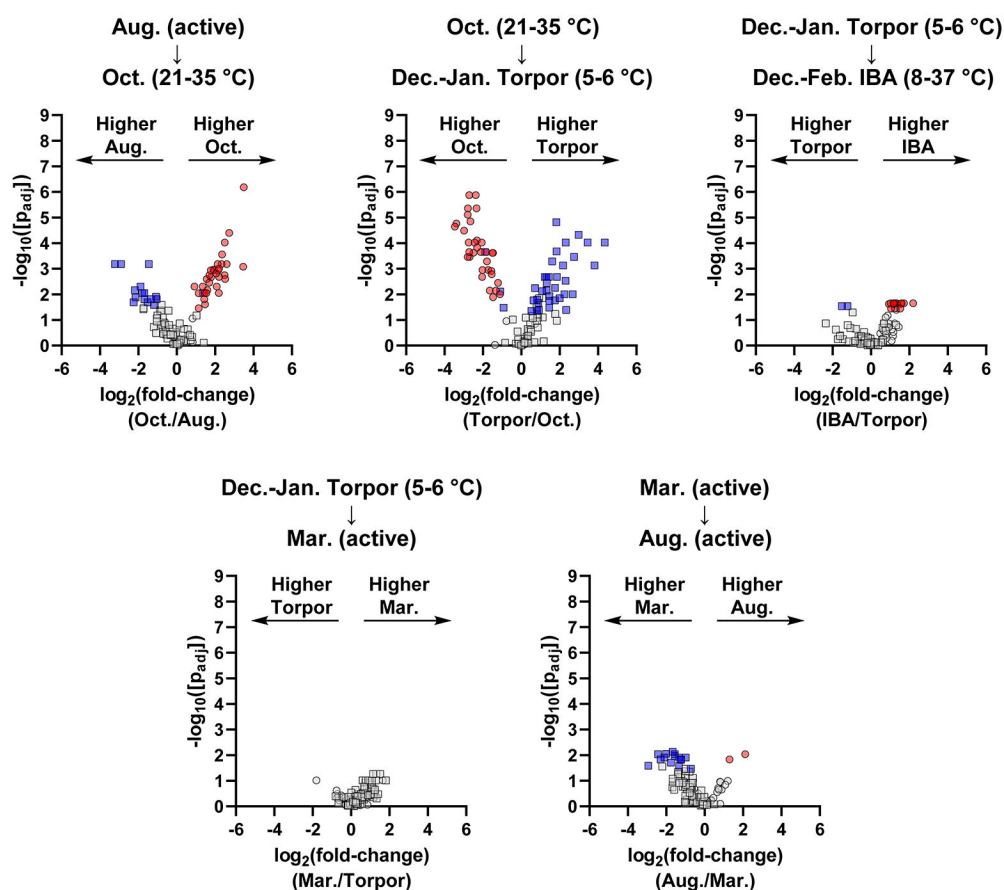


**Figure 4.**

Volcano plots representing pairwise comparisons for hypothalamus peptides for chronological transitions throughout the year. Circles represent prohormone-derived peptides, while squares indicate peptides arising from non-prohormone proteins. Red data points indicate significantly changing prohormone-derived peptides (passing both parametric and non-parametric tests with  $p < 0.05$ ). Blue data points indicate significantly changing non-prohormone derived peptides. Grey data points indicate peptides that were not significantly changing ( $p > 0.05$  in either or both tests).

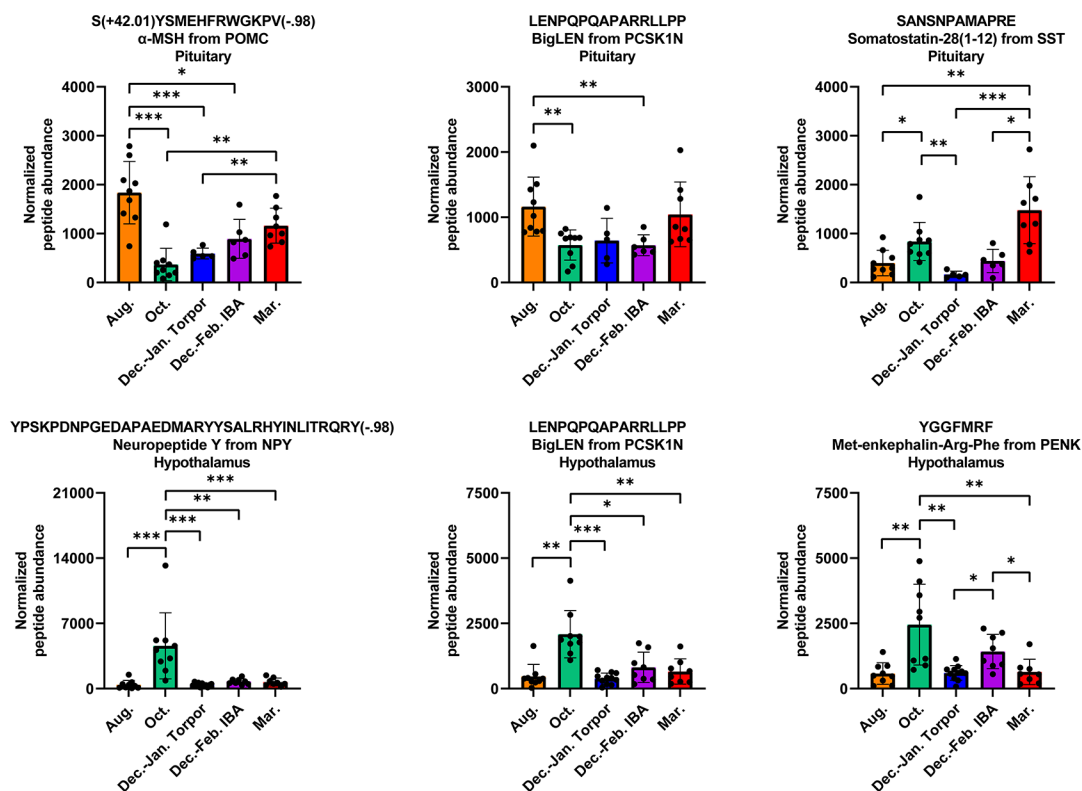


**Figure 5.**

Representative normalized abundances for selected peptides from the (top row) pituitary or (bottom row) hypothalamus. Each point represents the normalized peptide abundance for a given animal. Bars represent the mean  $\pm$  SD for each group. Post-translational modifications are indicated by mass change observed by mass spectrometry: amidation = (-.98), acetylation = (+42.01). Peptide abundances are considered statistically significant if they pass both parametric and non-parametric tests with  $p < 0.05$ , and  $p_{adj}$  is the minimum  $p$  value from these two tests. \* $p_{adj} < 0.05$ , \*\* $p_{adj} < 0.01$ , \*\*\* $p_{adj} < 0.001$ .

**Table 1.**

Significantly changing prohormone-derived pituitary peptides identified from the Oct. ( $T_b = 21-35\text{ }^\circ\text{C}$ ) vs. Aug. (Active) comparison.

Peptide Sequence <sup>a</sup>	Peptide Name <sup>b</sup>	Gene	FC(log2) <sup>c</sup>
EESESEEGTTSEVT		CHGB	2.03
GEAYHHVPESQRDKA		CHGB	1.49
EEASLQDRQYASHHT		CHGB	1.41
GEAYHHVPESQRD		CHGB	1.23
LDQLLHY		CHGB	1.22
EEASLQDRQYASHHTTE		CHGB	0.56
ELDQLLHY		CHGB	1.17
Q(-17.03)KIAEKFSQ		CHGB	1.20
SPQLEDE		PENK	0.99
YGGFM(+15.99)RF	Met-enkephalin-Arg-Phe	PENK	0.93
MYEENS RDNPF		SCG2	0.79
FPTLGGSQDKSLHN		SCG3	0.42
TLGGSQDKSLHN		SCG3	1.64
SANSNPAM(+15.99)APRE	Somatostatin-28(1-12)	SST	2.14
SANSNPAMAPRE	Somatostatin-28(1-12)	SST	1.07
Peptide Sequence <sup>a</sup>	Peptide Name <sup>b</sup>	Gene	FC(log2) <sup>c</sup>
AGAPEPAEPMELAKPSA	Copeptin(25-41)	AVP	-4.12
LAGAPEPA	Copeptin(24-31)	AVP	-5.23
LGVLFNPPYDPLQWKSSRFE		CHGB	-1.28
Q(-17.03)YDRVAELDQLLHY	BAM-1745	CHGB	-1.85
AADQDLGPEAPPEGVLGA	PEN-18	PCSK1N	-0.97
AADQDLGPEAPPEGVLGAL	PEN-19	PCSK1N	-1.86
LENPQPAPARRLLPP	BigLEN	PCSK1N	-1.02
VKMALQQEGFD		PCSK2	-1.75
DDGPYRMEHFRWGSPPKD	$\beta$ -MSH	POMC	-2.11
KYVMGHFRWD	Lys- $\gamma$ -MSH(1-10)	POMC	-1.62
KYVMGHFRWDRF(-.98)	Lys- $\gamma$ -MSH	POMC	-2.33
RPVKVYPNGAEDES(+79.97)AESFPLEF	CLIP	POMC	-2.53
RPVKVYPNGAEDESAESFPLEF	CLIP	POMC	-1.97
S(+42.01)YSMEHFRWGKPV(-.98)	$\alpha$ -MSH	POMC	-2.32
SYSMEHFRWGKPV(-.98)	Desacetyl- $\alpha$ -MSH	POMC	-1.67
Y(+42.01)GGFM(+15.99)TSEKSQTPLVTLFKNAIIKNAH	Ac- $\beta$ -endorphin(1-27)	POMC	-3.27
Y(+42.01)GGFMTSEKSQTPLVTLFKNAIIKNA	Ac- $\beta$ -endorphin(1-26)	POMC	-3.98
Y(+42.01)GGFMTSEKSQTPLVTLFKNAIIKNAH	Ac- $\beta$ -endorphin(1-27)	POMC	-4.00
Y(+42.01)GGFMTSEKSQTPLVTLFKNAIIKNAHKKGQ	Ac- $\beta$ -endorphin(1-31)	POMC	-2.71
YGGFMTSEKSQTPLVTLFKNAIIKNA	$\beta$ -endorphin(1-26)	POMC	-1.22
YGGFMTSEKSQTPLVTLFKNAIIKNAH	$\beta$ -endorphin(1-27)	POMC	-1.32
SVNPYLQGGRLDNVV		SCG5	-0.73

<sup>a</sup>Post-translational modifications are indicated by mass change observed by mass spectrometry. Amidation = (-.98), oxidation = (+15.99), pyroglutamylation = (-17.03), acetylation = (+42.01), phosphorylation = (+79.97).

<sup>b</sup>Peptide common names inferred from analogy to well-annotated rat sequence.

<sup>c</sup>Fold-change values are given for Oct./Aug. comparison. A positive value indicates the peptide is higher abundance in Oct.

Author Manuscript

Author Manuscript

Author Manuscript

Author Manuscript

**Table 2.**

Significantly changing prohormone-derived pituitary peptides identified from the Aug. (Active) vs. March (Active) comparison.

Peptide Sequence <sup>a</sup>	Peptide Name <sup>b</sup>	Gene	FC(log2) <sup>c</sup>
AGAPEPAEPMELAKPSA	Copeptin(25-41)	AVP	2.01
LAGAPEPA	Copeptin(24-31)	AVP	4.54
VKMALQQEGFD		PCSK2	1.33
RPVKVYPNGAEDES(+79.97)AESFPLEF	CLIP	POMC	3.47
RPVKVYPNGAEDESAESFPLEF	CLIP	POMC	2.11
Y(+42.01)GGFM(+15.99)TSEKSQTPLVTLFKNAIIKNAH	Ac-β-endorphin(1-27)	POMC	2.16
Y(+42.01)GGFMTSEKSQTPLVTLFKNAIIKNA	Ac-β-endorphin(1-26)	POMC	3.82
Y(+42.01)GGFMTSEKSQTPLVTLFKNAIIKNAH	Ac-β-endorphin(1-27)	POMC	1.97
YGGFMTSEKSQTPLVTLFKNAIIKNA	β-endorphin(1-26)	POMC	1.03
YGGFMTSEKSQTPLVTLFKNAIIKNAH	β-endorphin(1-27)	POMC	1.37
Peptide Sequence <sup>a</sup>	Peptide Name <sup>b</sup>	Gene	FC(log2) <sup>c</sup>
EDREEASLQDRQYASHHT		CHGB	-1.65
EDREEASLQDRQYASHHTTE		CHGB	-1.52
EEASLQDRQYASHHT		CHGB	-1.98
EEASLQDRQYASHHTTE		CHGB	-1.27
FLGEAYHHVPE		CHGB	-1.23
FLGEAYHHVPESQ		CHGB	-1.33
FLGEAYHHVPESQRD		CHGB	-2.03
FLGEAYHHVPESQRDKA		CHGB	-2.12
GEAYHHVPESQRD		CHGB	-1.61
GEAYHHVPESQRDKA		CHGB	-2.28
LDQLLHY		CHGB	-2.20
LGEAYHHVPESQRD		CHGB	-2.47
Q(-17.03)KIAEKFSQ		CHGB	-1.60
Q(-17.03)KIAEKFSQR(-.98)		CHGB	-2.52
SQGGEPGAYLTPDTREE		CHGB	-0.70
SLDSPAGPAE		CRH	-1.80
Q(-17.03)HWSYGLRPG(-.98)	GnRH/Gonadoliberin-1	GNRH1	-1.08
SPQLEDEAKEL		PENK	-0.84
SPQLEDEAKELQ		PENK	-0.62
GPEFRDDGAEPGP(-.98)		POMC	-0.92
PEFRDDGAEPGP(-.98)		POMC	-1.10
MYEENSIRDNPF		SCG2	-0.91
FPTLGGSDKSLHN		SCG3	-1.17
TLGGSDKSLHN		SCG3	-2.20
SVNPYLQGQRL		SCG5	-2.59
SANSNPAMAPRE	Somatostatin-28(1-12)	SST	-1.89

<sup>a</sup>Post-translational modifications are indicated by mass change observed by mass spectrometry. Amidation = (-.98), oxidation = (+15.99), pyroglutamylation = (-17.03), acetylation = (+42.01), phosphorylation = (+79.97).

<sup>b</sup>Peptide common names inferred from analogy to well-annotated rat sequence.

<sup>c</sup>Fold-change values are given for Aug./Mar. comparison. A positive value indicates the peptide is higher abundance in Aug.

Author Manuscript

Author Manuscript

Author Manuscript

Author Manuscript



**Table 3.**

Significantly changing prohormone-derived hypothalamus peptides identified from the Oct. ( $T_b = 21-35\text{ }^\circ\text{C}$ ) vs. Aug. (Active) comparison.

Peptide Sequence <sup>a</sup>	Peptide Name <sup>b</sup>	Gene	FC(log2) <sup>c</sup>
Q(-17.03)EDAELQP		CARTPT	3.50
Q(-17.03)EDAELQPR		CARTPT	2.50
FLGEAYHHVPESQ		CHGB	2.19
FLGEAYHHVPESQRD		CHGB	2.20
LGVLFPYDPLQWKSSRFE		CHGB	1.15
Q(-17.03)YDRVAELDQLLHY	BAM-1745	CHGB	0.92
SSPETLISDLLMRESTENVPRTRLEDPSMW	C-terminal flanking peptide	NPY	2.52
YPSKPDNPGEDAPAEDMARYYSALRHYINLITRQRY(-.98)	Neuropeptide Y	NPY	3.46
AADQDLGPEAPPEGVLGA	PEN-18	PCSK1N	1.91
AADQDLGPEAPPEGVLGAL	PEN-19	PCSK1N	1.96
AADQDLGPEAPPEGVLGALL	PEN-20	PCSK1N	1.36
AADQDLGPEAPPEGVLGALLRV	PEN	PCSK1N	1.59
LENPQPQAPA	LittleLEN	PCSK1N	2.61
LENPQPQAPARRLLPP	BigLEN	PCSK1N	2.16
SLSAASPPMTEAGTPRRF	LittleSAAS	PCSK1N	1.78
SVPRGEAAGAVQELARALAHLLLEAERQE	BigGAV	PCSK1N	1.57
VKMALQQEGFD		PCSK2	1.14
YGGFLRKYP	$\beta$ -neoendorphin	PDYN	2.33
YGGFLRKYPK	$\alpha$ -neoendorphin	PDYN	1.70
MDELYPVEPEEEANGGEVL		PENK	1.70
MDELYPVEPEEEANGGEVLA		PENK	1.48
SPQLEDEAKEL		PENK	1.77
SPQLEDEAKELQ		PENK	2.05
VGRPEWWMYDQ		PENK	1.45
YGGFMRF	Met-enkephalin-Arg-Phe	PENK	2.09
YGGFMRGL	Met-enkephalin-Arg-Gly-Leu	PENK	2.14
EIGDEENSAKFPI(-.98)	Neuropeptide-glutamic acid-isoleucine	PMCH	1.44
ALNSVAYERNAMQNYE	C-terminal flanking peptide	TAC1	2.21
RPKPQQFFGLM(-.98)	Substance P	TAC1	1.54
ASWTREPLE		TRH	2.51
ASWTREPLEE		TRH	2.36
EDEAAWSLDRTQQ		TRH	2.74

<sup>a</sup>Post-translational modifications are indicated by mass change observed by mass spectrometry. Amidation = (-.98), pyroglutamylation = (-17.03).

<sup>b</sup>Peptide common names inferred from analogy to well-annotated rat sequence.

<sup>c</sup>Fold-change values are given for Oct./Aug. comparison. A positive value indicates the peptide is higher abundance in Oct.

**Table 4.**

Significantly changing prohormone-derived hypothalamus peptides identified from the Dec.-Jan. (IBA) vs. Dec.-Feb. (Torpor) comparison.

Peptide Sequence <sup>a</sup>	Peptide Name <sup>b</sup>	Gene	FC(log2) <sup>c</sup>
Q(-17.03)EDAELQPR		CARTPT	1.57
FLGEAYHHVPESQRD		CHGB	1.25
LGVLFPYDPLQWKSSRFE		CHGB	0.94
Q(-17.03)YDRVAELDQLLHY	BAM-1745	CHGB	1.03
YGGFLRKYP	β-neoendorphin	PDYN	1.24
MDELYPVEPEEEANGGEVL		PENK	1.72
MDELYPVEPEEEANGGEVLA		PENK	2.19
SPQLEDEAKEL		PENK	1.34
VGRPEWWM DYQ		PENK	1.60
YGGFMRF	Met-enkephalin-Arg-Phe	PENK	1.23
YGGFMRGL	Met-enkephalin-Arg-Gly-Leu	PENK	1.05
ALNSVAYERNAMQNY	C-terminal flanking peptide(1-15)	TAC1	1.21
ALNSVAYERNAMQNYE	C-terminal flanking peptide	TAC1	1.53
ASWTREPLE		TRH	1.18

<sup>a</sup>Post-translational modifications are indicated by mass change observed by mass spectrometry. Pyroglutamylation = (-17.03).

<sup>b</sup>Peptide common names inferred from analogy to well-annotated rat sequence.

<sup>c</sup>Fold-change values are given for IBA/Torpor comparison. A positive value indicates the peptide is higher abundance in IBA.